Article
Beitr. Phys. Atmosph., August 1991, p. 169–184
0005-8173/91/03 00169–16 $ 3.00/0
Vol. 64, No.3

A Simple Model of the Convective Boundary Layer over Wavy Terrain with Variable Heat Flux

Dedicated to Dr. rer. nat. M. E. Reinhardt on the occasion of his 65th birthday

by U. SCHUMANN

DLR, Institut für Physik der Atmosphäre, 8031 Oberpfaffenhofen, Germany

(Manuscript received July 1991; in revised form September 1991)

Abstract

A simple model is deduced to determine quasi analytically the mean coherent circulation within a convective boundary layer at zero mean wind over a wavy surface with spatially variing surface heat flux. For a flat surface with uniform heat flux Q from the surface into the boundary layer, the mean circulation is strongest at a wavelength $\lambda \cong 4$ H. Here, H is the depth of the boundary layer. Wavy terrain with surface amplitude $\delta < H$ and a heat flux which varies at amplitude $q < Q$ around its mean cause the strongest circulation at about the same wavelength. The mean circulation is amplified by a factor of about $1 + \delta/(2H) + q/(4Q)$. An increase in mean circulation causes a decrease in the turbulence fluctuations but strongly enhances the effective diffusivities. The circulation depends only weakly on the surface roughness height. These results agree with results obtained from large eddy simulations. A variation q/Q has about the same effect as a variation in surface temperature relative to the mean temperature difference between the surface (at roughness height) and the mixed layer. The model is used moreover to identify differences between bottom-up and top-down diffusion and to estimate the critical Rayleigh number for onset of laminar convection and the critical Reynolds number for transition to turbulent convection.

Zusammenfassung

Ein einfaches Modell der konvektiven Grenzschicht über welligem Untergrund mit variablem Wärmestrom

Für die mittlere, kohärente Zirkulation in der konvektiven Grenzschicht bei mittlerer Windstille wird ein einfaches Modell abgeleitet, mit dem der Einfluß von welligem Untergrund und räumlich variierendem Wärmestrom an der Oberfläche nahezu analytisch bestimmt werden kann. Bei ebener Oberfläche mit konstantem Wärmestrom Q von der Oberfläche in die Grenzschicht ist die mittlere Zirkulation am stärksten bei einer Wellenlänge $\lambda \cong 4$ H ausgeprägt, wobei H die Grenzschichtdicke ist. Welliger Untergrund mit Amplitude $\delta < H$ oder ein mit Amplitude $q < Q$ variierender Wärmestrom verstärken die Zirkulation am stärksten bei etwa der gleichen Wellenlänge und zwar um etwa den Faktor $1 + \delta/(2H) + q/(4Q)$. Mit zunehmender mittlerer Zirkulation nimmt die Intensität turbulenter Bewegungen ab. Zugleich nimmt die effektive Diffusivität stark zu. Der Einfluß von Oberflächenrauhigkeiten auf diese Zirkulation ist gering. Diese Ergebnisse stimmen weitgehend mit Ergebnissen aus Grobstruktursimulationen überein. Die Variation von q/Q hat den gleichen Effekt wie eine räumliche Variation der Oberflächentemperatur relativ zur mittleren Temperaturdifferenz zwischen Oberfläche (in Höhe der Rauhigkeit) und Mischungsschicht. Das Modell wird zudem zur Erkennung von Unterschieden zwischen aufwärts und abwärts gerichteter Diffusion sowie zur Abschätzung der kritischen Rayleigh-Zahl für das Einsetzen laminarer Konvektion sowie der kritischen Reynolds-Zahl für turbulente Konvektion benutzt.

1 Introduction

The effects of surface inhomogeneities on the structure of the atmospheric boundary layer, the related surface fluxes of heat and momentum, their parameterization and remote sensing are subject of intensive research within the World Climate Research Programme (Becker et al., 1988). In this paper, we investigate the effects of variable surface heat flux and variable terrain height on the amplitude and scales of motion and on the related turbulent transports in the dry convective boundary layer (CBL), see Stull (1988). We assume zero or very weak mean wind and assume that the CBL is capped by a strong inversion so that vertical fluxes are vanishing at the top of the mixed layer.

It is well-known to glider pilots (Reinhardt, 1985) that wavy and thermally inhomogeneous terrain induces a

regular convective flow structure with updrafts above hills or relatively warmer surfaces. However, field observations of the structure of the atmospheric CBL, by Kaimal et al. (1982), Druilhet et al. (1983), Jochum (1988), and Huynh et al. (1990) found that "gently rolling terrain" affects the turbulence only little. Wilczak and Phillips (1986) found larger vertical velocity variance in particular in the upper CBL over the same terrain investigated by Kaimal et al. (1982), presumably because of shear induced by upslope flow and advection (J. Wilczak, personal communication, 1991). Hence, these experimental findings are about consistent. But the experimental studies did not explain why the effects of terrain appear to be small in most respect.

The case of periodic horizontal disturbances has been investigated analytically for laminar subcritical convection by Kelly and Pal (1978). Their linear analysis shows that the case with periodic temperature variation at flat walls is closely related to the constant temperature but undulated surface problem. Fully turbulent convection has been investigated by means of large-eddy simulation (LES). For example, the flow field in a convective boundary layer at weak mean winds has been determined for homogeneous surfaces by Schmidt and Schumann (1989). It was found that the lengthscale of spectral maximum of vertical velocities inside the mixed layer is about 1.5 H, in close agreement with experimental results by Caughey and Palmer (1979) and Kaimal et al. (1982). This lengthscale is determined from horizontal spectra of vertical velocity which are multiplied with wavenumber. As a consequence, this scale is smaller than the mean distance between the most energetic updrafts and downdrafts which is of order 2 to 4 H (Schmidt and Schumann, 1989; Krettenauer and Schumann, 1991; Moeng and Schumann, 1991). The average distance between all updrafts and downdrafts is smaller and of order H (Schumann and Moeng, 1991a). Laminar Rayleigh-Benard convection above a surface with prescribed temperature sets in at critical lengthscales of the order 2 H (Fiedler, 1989; Krettenauer, 1991). (As discussed in the appendix, larger lengthscales arise over surfaces with prescribed heat flux.) However, Priestley (1962) and Ray (1965) have shown that anisotropic turbulence with stronger horizontal than vertical mixing increases the horizontal scale of the convection. Since such anisotropies are typical for turbulent boundary layers, turbulent convection shows a little larger horizontal scale than laminar cases.

The effects of inhomogeneous surface heating on the turbulent CBL over a flat surface has been investigated using LES by several authors. Hadfield (1988) observed a general increase of velocity fluctuations due to an idealized two-dimensional surface heat-flux perturbation. Schmidt (1988) found considerable increase of horizontal velocity fluctuations with increasing inhomogeneity but a small reduction in the vertical velocity component. Graf and Schumann (1991) supported this result from simulations in comparison with field observations including a weak mean wind. Hechtel et al. (1990) simulated an observed case of the CBL with weak mean wind including moisture effects and random surface properties; they found little influence of inhomogeneity on the turbulence statistics. Schädler (1990) found larger effects from variations in surface moisture variations at scales of the order 10 to 20 km using two-dimensional simulations. On the other hand, Garratt et al. (1990) found "barely significant" changes in simulations of a sea breeze by random changes in surface temperature and surface roughness, when using a two-dimensional model with horizontal grid spacing of 7.5 km.

As a demonstrative example of the effect of inhomogeneous surface heating, Figure 1 shows results of a LES of a CBL with zero mean wind and with periodically varying surface heating. The simulation parameters are as given in Schmidt and Schumann (1989) except that the surface heat flux varies in a step-wise manner. It amounts to (2/3) Q for $0 \le x \le 2.5$ H, but to (4/3) Q for $2.5\ H \le x < 5$ H. Here Q is the mean heat flux and H the

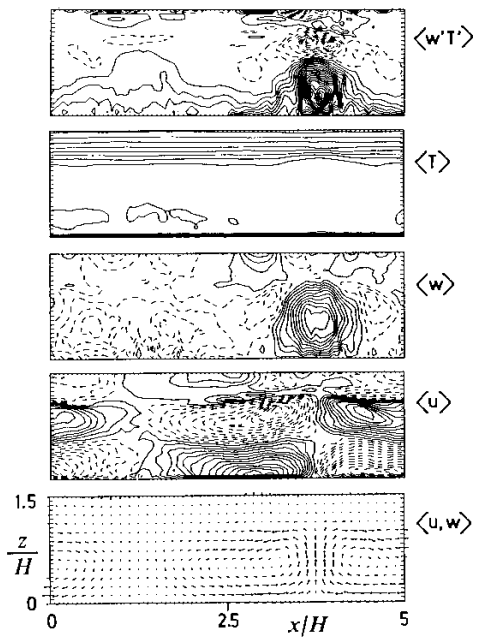

Figure 1 Mean flow field in a vertical cross-section of a CBL over a flat surface with step-wise varying surface heat flux. The panels show, from bottom to top: velocity vector field, horizontal velocity (contour increment 0.1 w_*), vertical velocity (0.1 w_*), potential temperature (8 T_*), vertical heat flux (0.2 Q). Here $Q = w_* T_*$ is the horizontal mean of the surface heat flux; q/Q = 2/3.

depth of the CBL. The resultant mean fields shown in Figure 1 represent averages over all grid points along the y coordinate. We observe a strong coherent circulation pattern. In terms of the convective velocity scale w_*, the maximum updraft/downdraft velocities are 1.02/ – 0.4 w_*, respectively, the maximum horizontal velocity is 1.32 w_*. The updraft deforms the stable layer above the mixed layer only slightly. The resultant heat flux is strongly concentrated and reaches a local maximum of 4.44 Q. In spite of the strong local updraft, the mean vertical velocity variance $\overline{w'^2}$, averaged over the x coordinate, is slightly smaller than for the corresponding homogeneous case with constant surface heating; the maximum value of $\overline{w'^2}/w_*^2$ is 0.40/0.43 in the inhomogeneous/homogeneous cases, respectively. However, the horizontal velocity variance increases over the inhomogeneous surface; the maximum mean values of $\overline{u'^2}/w_*^2$ occur near the bottom surface and amount to 0.57/0.32 in the two cases, respectively.

Turbulent convection over wavy terrain has been investigated by Krettenauer and Schumann (1989b), Walko et al. (1990), and Krettenauer and Schumann (1991). The latter have presented figures similar to Figure 1. It was shown that the motion structure reacts most strongly to surface inhomogeneities at the wavelength of the most dominant coherent structure which exists also over homogeneous surfaces. This suggests the existence of "resonant" convection (Kelly and Pal, 1978). However, a simple explanation of this scale selection is not yet known.

As demonstrated by Egger (1987), very simple models may be helpful to explain the basic properties of buoyancy driven flows in rather complex cases like valley-plain circulations. In this paper, an even simpler model is deduced which, as we will see, explains quasi analytically many of the previous findings on the scale and motion amplitudes of convection over inhomogeneous terrain. The model is described in Section 2. In that section it is assumed for simplicity that the turbulent diffusivities can be prescribed. Section 3 deduces the solutions, and Section 4 discusses the results of this model. For comparisons, the same model is also applied to laminar flow cases for which the solutions are given in the Appendix. In Section 5, we refine the turbulence model in that we deduce the amplitude of turbulent motions (in contrast to the coherent motion part of the mean circulation) from the budget of kinetic energy. This will also explain variations of turbulent fluctuations as a function of the forcing and of the scales of the coherent motion part. Section 6 investigates the equivalence of variations in surface heat flux and temperature variations. The effective diffusivities for mixing within the CBL in vertical and horizontal directions and for bottom-up and top-down diffusion are deduced in Section 7. Finally, Section 8 summarizes and discusses the results.

2 The Model

We consider the turbulent convection in a boundary layer of mean depth H driven by a mean surface temperature flux Q at zero mean wind. The surface is assumed to have a regular wavy form with wavelength λ and amplitude $\delta < H$. The surface heat flux varies also periodically with the same wavelength and amplitude $q < Q$ around the positive mean value Q. We assume that all properties vary piecewise linearly. The resultant mean deviations in the heat fluxes are $\pm q/2$. In the case of Figure 1, $q/Q = 2/3$. The surface is assumed to be rough with roughness height z_0 (we take equal values for momentum and heat transfer, for simplicity). The top of the boundary layer is assumed to be represented by a very stable inversion such that it can be approximated by a rigid free-slip adiabatic boundary. The fluid is exposed to gravity g. We assume the Boussinesq approximation for a fluid with uniform density ρ, and constant volumetric expansion coefficient $\beta = -(\partial\rho/\partial T)/\rho$; $\beta = 1/\overline{T}$ in air. Because of constant mean surface heating, the volume averaged temperature $\overline{T}$ increases at constant rate

$$d\overline{T}/dt = Q/H\,. \tag{1}$$

In order to obtain an estimate of the resultant convective (coherent) motions we approximate the flow domain, as sketched in Figure 2, by four subdomains, 1 to 4, each of width $b = \lambda/4$. On average the depth of the subdomains is $h = H/2$. Between the subdomains, we assume a flow with surface averaged velocities u from domain 1 to domain 2, and, for continuity, at the same rate from domain 3 to 4. In the vertical directions the corresponding flow velocities from 2 to 3 and from 4 to 1 have the mean value w. Flow across other boundaries of the subdomains are zero because of symmetry, periodicity and because of top and bottom boundary conditions. Because of continuity,

$$u\,h = w\,b\,. \tag{2}$$

This equation applies for arbitrary values of $\delta < H$ because the velocities are the Cartesian components and because the domain height is 2 h at the mid-interface

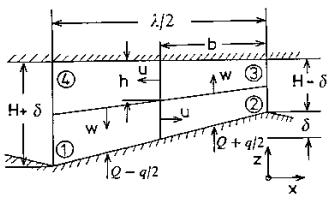

Figure 2 Sketch of a half-wave (wavelength $\lambda = 4b$) of a vertical cross-section of the periodic flow domain of mean height $H = 2h$ with surface height amplitude δ and mean variations in surface temperature flux $Q \pm q/2$, showing the four control volumina 1 to 4, and characteristic horizontal and vertical velocities u and w. The domain extends infinitely in the homogeneous direction y normal to the depicted cross-section.

for symmetry. The volume sizes of the four subdomains, per unit length in y direction, are

$$V_1 = V_4 = b\,(h + \delta/4),\quad V_2 = V_3 = b\,(h - \delta/4). \quad (3)$$

Let T_i, i = 1, 2, 3, 4, denote the mean local temperature deviations from the (arbitrary) mean temperature $\overline{T}$. We approximate advective fluxes by "upstream" values, e.g. the flux from volume 1 to volume 2 equals $h\,u\,T_1$. In contrast to central differences this introduces some finite mixing even for zero diffusive fluxes but guarantees meaningful solutions for arbitrary magnitude of the velocities (Spalding, 1972). Without loss of generality, this requires $u \geq 0$. Moreover, we apply Eq. (2). Then, the heat balance for each of the subdomains results in

$$V_1 \frac{dT_1}{dt} = -(uh + w'b)(T_1 - T_4) - u'h\,(T_1 - T_2) + (Q - q/2)\,b - V_1 \frac{d\overline{T}}{dt}, \quad (4)$$

$$V_2 \frac{dT_2}{dt} = -(uh + u'h)(T_2 - T_1) - w'b\,(T_2 - T_3) + (Q + q/2)\,b - V_2 \frac{d\overline{T}}{dt}, \quad (5)$$

$$V_3 \frac{dT_3}{dt} = -(uh + w'b)(T_3 - T_2) - u'h\,(T_3 - T_4) - V_3 \frac{d\overline{T}}{dt}, \quad (6)$$

$$V_4 \frac{dT_4}{dt} = -(uh + u'h)(T_4 - T_3) - w'b\,(T_4 - T_1) - V_4 \frac{d\overline{T}}{dt}. \quad (7)$$

Here, u′ and w′ are effective turbulence velocities such that, e.g., $w'(T_1 - T_4) = -K_v(T_4 - T_1)/h$, describes the turbulent flux density between volumes, e.g. from 1 into 4. They are related to horizontal and vertical diffusivities,

$$K_h = u'b \quad \text{and} \quad K_v = w'h, \quad (8)$$

respectively. Below, the same diffusivities are used for momentum transport, i.e. the turbulent Prandtl number is assumed to be equal to one.

The horizontal momentum balance is set up for a control volume of size $V_u = b\,h$ enclosing either the lower or the upper lateral interfaces between volumes 1 and 2 and between 3 and 4. The shear stress at the bottom surface is denoted by $-u_*^2$ as a function of the friction velocity u_*. To first order in geometrical terms, the balances are

$$V_u \frac{du}{dt} = (p_1 + u^2/4)(h + \delta/4) - (p_2 + u^2/4)(h - \delta/4) + (p_1 + p_2 + p_3 + p_4)\,\delta/8 - p_s\delta - 2w'ub - u_*^2 b, \quad (9)$$

for the lower of the two volumes V_u, and

$$V_u \frac{du}{dt} = (p_3 + u^2/4)(h - \delta/4) - (p_4 + u^2/4)(h + \delta/4) + (p_1 + p_2 + p_3 + p_4)\,\delta/8 - 2w'ub. \quad (10)$$

for the upper volume. Here p_i is the mean pressure (per unit mass) in the i-th control volume; p_s is the pressure at the bottom surface of the lower domain V_u. The first two terms on the right of the equations measure the pressure force and the advection at the lateral boundaries of the control volume. The next terms describe horizontal acceleration due to pressure forces on the inclined upper and lower surfaces of the subdomain. The last terms account for vertical diffusive fluxes. Horizontal diffusion of horizontal momentum is assumed to be small in comparison to the advective parts and neglected therefore. By hydrostatic approximation, to first order in geometrical terms,

$$p_s = (p_1 + p_2)/2 - \beta g\,(T_1 + T_2)\,h/4. \quad (11)$$

Similarly, the vertical momentum balance is formulated for the two control volumina enclosing the interface between subdomains 2 and 3 and 4 and 1. The left of these has the size V_1, the right one has the size V_2:

$$V_1 \frac{dw}{dt} = (p_4 - p_1)\,b - \beta g\,(T_1 + T_4)\,V_1/2 - 2u'h\,w, \quad (12)$$

$$V_2 \frac{dw}{dt} = (p_2 - p_3)\,b + \beta g\,(T_2 + T_3)\,V_2/2 - 2u'h\,w. \quad (13)$$

Here, the last term describes lateral mixing of vertical momentum, which is a non-hydrostatic effect. The vertical advection $bw^2/4$ is equal on the upper and lower boundary of the control volume and drops out, therefore. Again, diffusion in the direction of the flow is neglected.

To close the set of equations, we have to specify the turbulent diffusivities K_h, K_v, and the surface friction velocity u_*. The latter is related to the horizontal flow velocity u according to the Monin-Obukhov relationships, following Paulson (1970) and Dyer (1974):

$$u = \frac{u_*}{\kappa}\left[\ln(z/z_0) - \psi_m(z/L) + \psi(z_0/L)\right], \quad (14)$$

$$\psi_m(\zeta) = 2\ln\left[(1 + \varphi_m^{-1})/2\right] + \ln\left[(1 + \varphi_m^{-2})/2\right] - 2\arctan(\varphi_m^{-1}) + \frac{\pi}{2}, \quad (15)$$

$$\varphi_m(\zeta) = (1 - 16\zeta)^{-1/4},\quad L = -u_*^3/(\kappa\beta g Q),\quad \kappa = 0.41. \quad (16)$$

These equations apply to the unstable case, i.e. for $Q \geq 0$, where the Obukhov-length L is negative. They are evaluated for z = h/2. Although strictly justified for homogeneous boundary layers only, Tsvang et al. (1991)

have shown that these relationships pertain also to non-homogeneous surfaces.

The turbulent diffusivities are roughly approximated by

$$K_h = 3\alpha v' h, \quad K_v = \alpha v' h, \tag{17}$$

so that, see Eq. (8),

$$u' = 3\alpha v' h/b, \quad w' = \alpha v'. \tag{18}$$

Here, $\alpha \cong 0.1$ and $K_h/K_v \cong 3$ are empirical parameters. The impact of these assumptions will be discussed below. In this section, we approximate the controlling turbulence velocity by

$$v' = (w_*^2 + 4u_*^2)^{1/2}, \quad w_* = (\beta g H Q)^{1/3}, \tag{19}$$

where w_* is Deardorff's convective velocity scale and v' one possible form of a scaling velocity for sheared convection, proposed by Penc and Albrecht (1987). An alternative method to determine v' will be described in Section 5.

3 Solutions

For steady state, i.e. $dw/dt = 0$, Eqs. (12), (13) with Eq. (2), determine the pressure differences

$$p_4 - p_1 = \beta g (T_1 + T_4)(h + \delta/4)/2 + 2u'uh^2/b^2, \tag{20}$$

$$p_3 - p_2 = \beta g (T_2 + T_3)(h - \delta/4)/2 - 2u'uh^2/b^2. \tag{21}$$

The sum of Eqs. (9) and (10) gives

$$2V_u \frac{du}{dt} = (p_1 + p_3 - p_2 - p_4)h + \\ + (p_1 + p_2 - 2p_s)\delta/2 - 4w'ub - u_*^2 b. \tag{22}$$

Using Eqs. (11), (20), and (21) results in

$$2V_u \frac{du}{dt} = -(4u'h^3/b^2 + 4w'b)u - u_*^2 b + \\ + \beta g[(T_2 + T_3 - T_1 - T_4)h^2/2 - \\ - (T_3 - T_2 + T_4 - T_1)h\delta/8]. \tag{23}$$

For steady state, i.e. $dT_i/(dt) = 0$, Eqs. (4)–(7) together with (1) result in

$$T_1 - T_4 = -\mu(T_1 - T_2) + W_1;$$

$$W_1 = \frac{b\{1 - \delta/(4h) - q/Q\}Q}{2(uh + w'b)}, \tag{24}$$

$$T_2 - T_1 = -\nu(T_2 - T_3) + W_2;$$

$$W_2 = \frac{b\{1 + \delta/(4h) + q/Q\}Q}{2h(u + u')}, \tag{25}$$

$$T_2 - T_3 = \mu(T_3 - T_4) + W_3;$$

$$W_3 = \frac{b\{1 - \delta/(4h)\}Q}{2(uh + w'b)}, \tag{26}$$

$$T_3 - T_4 = \nu(T_4 - T_1) + W_4;$$

$$W_4 = \frac{b\{1 + \delta/(4h)\}Q}{2h(u + u')}, \tag{27}$$

where

$$\mu = \frac{h}{b}\frac{u'}{w + w'}, \quad \nu = \frac{b}{h}\frac{w'}{u + u'}. \tag{28}$$

This set of linear equations can be solved to obtain the temperature differences

$$T_4 - T_1 = D^{-1}(-W_1 - \mu W_2 + \mu\nu W_3 + \mu^2\nu W_4), \tag{29}$$

$$T_1 - T_2 = D^{-1}(-W_2 + \nu W_3 + \mu\nu W_4 - \mu\nu^2 W_1), \tag{30}$$

$$T_2 - T_3 = D^{-1}(W_3 + \mu W_4 - \mu\nu W_1 - \mu^2\nu W_2), \tag{31}$$

$$T_3 - T_4 = D^{-1}(W_4 - \nu W_1 - \mu\nu W_2 + \mu\nu^2 W_3). \tag{32}$$

The solutions exist since the determinant

$$D = 1 - \mu^2\nu^2 = (1 - \mu\nu)(1 + \mu\nu), \tag{33}$$

stays positive, because of the usage of upstream differences, even for $u' = w' = 0$ if $u > 0$. Hence, the required vertical and horizontal temperature differences are

$$T_2 - T_3 + T_1 - T_4 = \frac{Q[u(2 - \delta/H - q/Q) + 4u']}{w(u + u') + w'(u + 2u')}, \tag{34}$$

and

$$T_2 + T_3 - T_1 - T_4 = \\ = \frac{\lambda Q[w(2 + \delta/H + q/Q) + 2w'(\delta/H + q/Q)]}{4H[w(u + u') + w'(u + 2u')]}. \tag{35}$$

Finally, inserting the temperature differences into Eq. (23) and normalizing with w_*, Eq. (19), gives

$$\frac{H}{w_*^2}\frac{du}{dt} = -4\left(\frac{8u'}{w_*}H^3/\lambda^3 + \frac{w'}{w_*}\right)\frac{u}{w_*} - u_*^2/w_*^2 + \\ + \frac{w_*[2w + (w + 2w')(\delta/H + q/Q)]}{8[w(u + u') + w'(u + 2u')]} + \\ + \frac{w_*[4u' + u(2 - \delta/H - q/Q)]\,\delta/\lambda}{8[w(u + u') + w'(u + 2u')]}. \tag{36}$$

For steady state ($du/dt = 0$), the solution u/w_* of this equation for given values of $\lambda/H = 2b/h$, $\delta/H = \delta/(2h)$, q/Q, and for given z_0/H can be determined iteratively by solving

$$\frac{u}{w_*} = -x' + \sqrt{x'^2 + r}, \quad \text{where } x' = \frac{u'}{2w_*}, \tag{37}$$

with

$$r = \frac{(u + u')[2w + (w + 2w')(\delta/H + q/Q)]}{8\{4[8(u'/w_*)H^3/\lambda^3 + w'/w_*] + C_d u_*/w_*\}m} + \\ + \frac{(u + u')[4u' + u(2 - \delta/H - q/Q)]\,\delta/\lambda}{8\{4[8(u'/w_*)H^3/\lambda^3 + w'/w_*] + C_d u_*/w_*\}m} \tag{38}$$

with $m = [w(u + u') + w'(u + 2u')]$.

Here $w = 2uH/\lambda$ and $C_d = u_*/u$ is the drag coefficient given by the solution using Eq. (14). In the iteration which is used to evaluate the above solution, one has to make sure that the solutions get nonnegative. This is important in particular for homogeneous surfaces with $\delta = q = 0$, because in this case a positive solution exists only for $\lambda > \lambda_{crit}$, see below.

4 Discussion

4.1 Limiting Analytical Results

The model equations show that the normalized surface undulation amplitude δ/H and the relative change in heat flux q/Q control the response to surface inhomogeneities. The importance of surface inhomogeneities depends on the wavelength λ/H. In order to get some insight in the model's solutions we first consider the cases of very large or very small wavelengths. For the limiting case of $\lambda/H \to \infty$, $u'/w_* \to 0$, compare Eq. (18), and therefore

$$\frac{u}{w_*} = \frac{1}{2}\sqrt{\frac{q/Q + \delta/H}{4w'/w_* + C_d u_*/w_*}}, \quad \frac{w}{w_*} \to 0. \quad (39)$$

In this limit, variations by δ/H and q/Q have equivalent effects. One obtains a finite coherent circulation which magnitude depends strongly on the vertical turbulence velocity w' and also on the friction velocity u_*. Obviously, the smaller the turbulence velocity scales are the stronger is the large-scale convection. Since $C_d < 1$, surface friction will in general be less important than the convective turbulence in limiting the coherent motions.

In the other extreme, for very short wavelengths, $\lambda/H \ll 1$, we obtain $u \ll u'$, $w \ll w'$, $C_d \to 0$, and

$$\frac{u}{w_*} = \frac{1}{18432}\frac{1}{\alpha^2}\frac{\lambda^5}{H^5}\left(\delta/H + q/Q + 24\frac{H}{\lambda}\frac{\delta}{\lambda}\right). \quad (40)$$

Here, the terms containing δ vanish over smooth terrain where δ/H goes to zero faster than $(\lambda/H)^2$. The result suggests zero motions over homogeneous terrain and a strong dependence on α, i.e. on turbulent diffusion.

However, this solution is valid only for very small motion amplitudes. Since, as we will see below, u gets quickly larger than u', in particular for finite inhomogeneity, we also have a range where $w' \ll u$, $u' \ll u$, and λ/H of order unity, for which we find

$$\frac{u}{w_*} = \sqrt{\frac{1 + \delta/H + q/(2Q) - (\delta/H + q/Q)\,\delta/(4H)}{16\,(48H^4/\lambda^4 + 1)\,\alpha + 4C_d u_*/w_*}},$$

$$w = u\frac{2H}{\lambda}, \quad (41)$$

i.e. larger values for small λ/H and a weaker dependence on α. The weaker dependence on α for large motion amplitudes reveals the fact that the convective circulation is only partly limited by turbulent mixing. In fact it is limited mainly by the amount of heat available to drive the circulation, i.e. by w_*. This result shows also that the surface friction plays the smaller role in comparison to the convective turbulence in limiting the coherent motions. Moreover, we note the nonlinear interaction of undulation and variable heat flux. If both types of inhomogeneity are present, the coherent circulation induced by variable surface heating gets reduced over wavy terrain. The results for the limiting cases of large and small wavelengths together show the existence of a wavelength λ_{max} with maximum coherent motion.

For a wavelength of order 4 H, for $C_d \ll 1$, and for small inhomogeneities, Eq. (41) reduces to the simple result

$$\frac{u}{w_*} \cong A\left[1 + \frac{\delta}{2H} + \frac{q}{4Q}\right], \quad w = \frac{u}{2}. \quad (42)$$

Here, $A \cong 1.0$ for $\alpha = 0.05$, and $A \cong 0.7$ for $\alpha = 0.1$.

The limiting results for a homogeneous surface, i.e. $\delta = q = 0$, are easily derived from the above equations. We see that $u/w_* \to 0$ both for very small and very large wavelengths. As discussed in the Appendix, this is a noteworthy result because it deviates from the linear theory of convection which predicts onset of laminar convection over a uniformly heated surface at infinite wavelengths. Also the zero solution for homogeneous surface given by Eq. (40) is surprising. One may ask, when the solution gets positive. In fact, if we determine the general solution for $\delta = q = 0$, and for $u \ll u'$, $w \ll w'$, for which $C_d \ll 1$, we find

$$\frac{u}{w_*} = \frac{w_*}{8\,(2u' + w'\lambda/H)}$$
$$\left\{\left(8\frac{u'}{w_*}\frac{H^3}{\lambda^3} + \frac{w'}{w_*}\right)^{-1} - 16\frac{\lambda}{H}\frac{w'u'}{w_*^2}\right\}. \quad (43)$$

Obviously, a positive solution exists only if the last bracketed term is positive. This is the case if λ exceeds a critical wavelength λ_{crit}, where

$$\frac{\lambda_{crit}}{H} = \left[\frac{512\psi^2\alpha^3(v'/w_*)^3}{1 - 32\psi\alpha^3(v'/w_*)^3}\right]^{1/4}, \quad (44)$$

with $\psi \equiv K_h/K_v$. For $\psi = 3$, as assumed in this paper, and for $v' = w_*$, we get $\lambda_{crit}/H = 1.503$ if $\alpha = 0.1$, and $\lambda_{crit}/H = 0.874$ if $\alpha = 0.05$. To first order, λ_{crit} grows as $\psi^{1/2}$. Formally this kind of condition is similar to a critical Rayleigh number for the onset of laminar convection, see Appendix. However the present condition

means that narrow convection cells which span vertically over the whole layer depth get dissipated by lateral turbulent mixing. It does not mean that there is no turbulence at smaller scales.

4.2 Numerical Results for the General Cases

Figures 3 and 4 show the numerical solutions of Eq. (37) for cases with zero heat flux variations (full curves) and for cases with plane surfaces (dashed curves) and for various values of the inhomogeneity parameters, δ/H and q/Q, as a function of wavelength λ/H. The figures contain two sets of solutions, one for $\alpha = 0.1$, and one for 0.05. The numerical solutions clearly show the existence of a critical wavelength λ_{crit}, below which the motion amplitude is zero for $\delta = q = 0$. The value of this wavelength is as predicted by Eq. (44). The sudden transition does not arise for finite inhomogeneity; here the motion amplitude is finite even for subcritical wavelengths, see Eq. (40). As expected from Eq. (41), u increases strongly with decreasing α. Moreover, smaller values of α shift the wavelength λ_{crit} to larger values, whereas the wavelength λ_{max} is less sensitive to this parameter. Also an increase in the ratio $\psi = K_h/K_v$, which we assumed to be $\psi = 3$, causes an increase in these wavelengths with $\psi^{1/2}$, as suggested by Eq. (44). The same trend in the wavelength of maximum response was predicted before by Priestley (1962) and shown analytically by Ray (1965). From LES, we expect a coherent motion amplitude of order unity and a wavelength of order 4 H. Therefore, the selected ratio of diffusivity values and the values of α in between 0.05 and 0.1 appear to be realistic. Tests with other models for v', including $v' = w_*$, and $v' = w_* + 0.1u\,(1 + h/b)$, showed that such variations are unimportant.

Figure 3 shows that the coherent flow part achieves a broad maximum at a λ_{max} in between 4 and 7 H with respect to the horizontal component. The vertical one, see Figure 4, exhibits a more pronounced maximum between 2 and 3 H. We see that both inhomogeneity parameters increase the coherent circulation, but the circulation is quite large already for $\delta = q = 0$. The wavelength of maximum response increases slightly for increasing inhomogeneity parameters. The numerical results show the strong increase proportional to $(\lambda/H)^5$ for $\lambda/H < 0.1$, see Eq. (40), but proportional to $(\lambda/H)^2$ for larger values with $\lambda/H < 1$, as can be seen from Eq. (41). The results also show the tendency towards a finite asymptotic value at large wavelengths. This reduction becomes effective at large λ for which $w = 2uH/\lambda < w'$, so that w' dominates the vertical exchange, see Eq. (39). For small wavelengths we get similar responses for δ/H as for $q/(2Q)$. However for large wavelengths, equivalent responses are obtained for $\delta/H = q/Q$. The asymptotic value is zero for $\delta = q = 0$, compare Eq. (39). Further parameter studies have shown a very weak sensitivity to the surface roughness height; its effect is less than 4 % for $0 < z_0/H \leq 10^{-4}$.

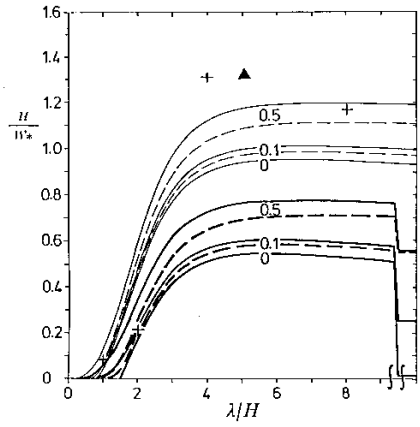

Figure 3 Horizontal convection velocity u/w_* versus wavelength λ/H for various values of terrain amplitude $\delta/H = 0, 0.1$, and 0.5, with $q/Q = 0$ (full curves), and for various values of surface heating $q/Q = 0, 0.1$, and 0.5, with $\delta/H = 0$ (dashed curves). Thick curves for $\alpha = 0.1$, thin curves for $\alpha = 0.05$, see Eq. (17). Asymptotic solutions for $\lambda/H = 1000 \cong \infty$ ($\alpha = 0.1$) are indicated at the right vertical axis. The crosses denote the LES results from Krettenauer and Schumann (1991) for $\delta/H = 0.1$ and $q/Q = 0$, the triangle represents the LES shown in Figure 1 with $\delta/H = 0$, $q/Q = 2/3$. In all cases, $z_0/H = 10^{-4}$.

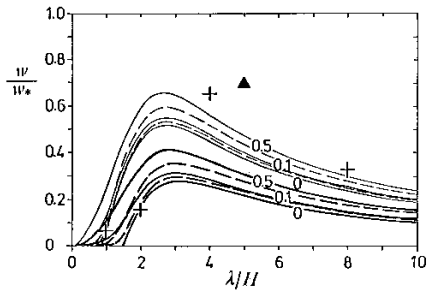

Figure 4 Same as Figure 3 for the vertical convection velocity w/w_* versus wavelength λ/H.

4.3 Comparisons with Numerical Results

As discussed in the introduction, LES results show that the characteristic distance between updrafts and the wavelength of maximum w-spectrum is of order 1.5 to 4 H for homogeneous surfaces. Also, the maximum root-mean-square value of the horizontal velocity fluctuations and the maximum value of u in conditional

plume averages is of order 0.7 w_*. Moreover, Krettenauer and Schumann (1989) found a maximum response to wavy terrain for $\lambda \cong 4$ H. These findings are in rough agreement with the prediction of the model for $\alpha = 0.1$ as shown in Figures 3 and 4. However, the figures show that the simple model underestimates the maximum response in motion amplitude for wavy terrain of amplitude $\delta/H = 0.1$, in comparison to the LES results. In this respect, the results for $\alpha = 0.05$ agree slightly better. The smallness of α indicates that turbulent mixing between updrafts and downdrafts is rather weak in comparison to the transports by coherent motions and this is consistent with the analysis of Schumann and Moeng (1991b). The rather strong sensitivity to α suggests that the false diffusion introduced in this model by upstream differences (Spalding, 1972) is relatively unimportant. On the other hand, as noted in Section 2, we have neglected turbulent diffusion in flow direction. Further analysis has shown that inclusion of this diffusivity causes a slower increase of u/w_* with λ/H and larger wavelengths of maximum response so that the results agree less with the LES results. The present model predicts about the same magnitude as the LES over wavy terrain and over flat terrain with variable heat flux. The model even explains approximately the appearance of a sudden transition from small to large circulation amplitudes in the LES. However, the maximum of response near $\lambda/H = 4$ is more pronounced in the LES than in the model. We note that the LES results refer to the maximum values of u/w_*, where u denotes the local maximum of the mean horizontal circulation velocity, whereas the present theory predicts an average velocity u within a volume of size $(H/2) \cdot (\lambda/4)$. The LES results shown by the symbols in Figure 4 represent the average of the updraft and the downdraft velocity magnitudes. The triangle reflects a rather strong reaction which is reasonable in view of the large value of the inhomogeneity parameter, $q/Q = 2/3$, of this case, whereas the crosses apply to $\delta/H = 0.1$. The simple model predicts equal velocities for updrafts and downdrafts which, in reality, are quite different. Moreover, the simple model excludes variations on smaller scales which may react more strongly. Figure 1 shows that the updraft is quite narrow while the downdraft is much wider. Hence we cannot expect complete agreement. However, both the LES and the present model agree in predicting approximately the same trends in velocity magnitude. In view of the differences between the LES and the model, the agreement appears to be satisfactory. The present model predicts the mean circulation magnitude up to a factor of about two.

4.4 Vertical and Horizontal Temperature Differences

The temperature differences are given in Eqs. (34) and (35). We note that the differences are finite even for $u' = w' = 0$,

$$\frac{T_2 - T_3 + T_1 - T_4}{2} = \frac{Q\,(2 - \delta/H - q/Q)}{2w} \cong \frac{2}{A} T_* \left(1 - \frac{\delta}{H} - \frac{3}{4}\frac{q}{Q}\right), \tag{45}$$

$$\frac{T_2 + T_3 - T_1 - T_4}{2} = \frac{\lambda Q\,(2 + \delta/H + q/Q)}{4Hu} \cong \frac{2}{A} T_* \left(1 + \frac{q}{4Q}\right), \tag{46}$$

where the latter relations apply for $\lambda = 4$ H, $T_* = Q/w_*$. The temperature differences are finite because the essential mixing is implicit in the model which assumes a given flux of heat from the surface without considering the details of the heat transfer process. The heat input causes the increase in mean temperature within the layer. Both processes are independent of the turbulent mixing inside the mixed layer. This explains also why false diffusion by finite difference errors in the model is relatively unimportant.

Eq. (46) predicts a mean temperature difference of about 2 to 3 T_*. From LES and measurements (Schumann and Moeng, 1991a), this value varies between 3.2 T_* near the surface and zero at the top of the mixed layer. Hence, the simple model gives about the correct magnitude.

5 Energetics of Coherent and Turbulent Motion Parts

In the previous section the turbulent velocity scale v' was assumed to be a given function of w_* and u_*, see Eq. (19). In this section, v' will be estimated from the budget of turbulent kinetic energy. The total kinetic energy $E_{tot} = E + e$, averaged over the whole domain, is composed of the energy $E = \gamma\,(u^2 + w^2)/2$ of the coherent motion part plus $e = 3\,v'^2/2$, the turbulent motion part. The factor γ measures the ratio between the averaged energy of the coherent motion and its maximum value. For a linear variation of the velocities within the four subdomains, as it is consistent with the present model concept, we have $\gamma = 1/3$. The total energy satisfies

$$\frac{d}{dt}(E + e) = \frac{1}{2}\beta g Q - \varepsilon\,, \tag{47}$$

where the source term describes the energy production due to buoyancy and ε is the viscous dissipation rate.

The factor 1/2 enters the buoyant part because the mean heat flux decreases from its surface value to zero at the top and equals Q/2 on average. Shear contributions from the coherent motions are irrelevant in this sum, because shear production of turbulent motions equals shear energy loss of coherent motions. Also diffusion and pressure contributions vanish because they are zero in the volume mean for the given boundary conditions. The energy of the coherent motion part satisfies

$$\frac{d}{dt} E = \gamma \left(u \frac{du}{dt} + w \frac{dw}{dt} \right) = \gamma u \frac{du}{dt} (1 + h^2/b^2), \qquad (48)$$

where the last relation comes from continuity. The difference of Eqs. (47) and (48), normalized by w_*, see Eq. (19), gives

$$\frac{H}{w_*^3} \frac{d}{dt} e = \frac{1}{2} - \frac{H\varepsilon}{w_*^3} - \gamma \frac{u}{w_*} \frac{H}{w_*^2} \frac{du}{dt} (1 + 4H^2/\lambda^2). \qquad (49)$$

The acceleration term du/dt is given by Eq. (36). The dissipation rate ε is commonly related to the turbulence velocities by

$$\varepsilon = \frac{e^{3/2}}{L_\varepsilon} = \frac{(3 v'^2/2)^{3/2}}{L_\varepsilon}, \qquad (50)$$

where L_ε is the dissipation lengthscale. For the homogeneous case and vanishing coherent motions, e comprises the total kinetic energy. For this case, Krettenauer and Schumann (1991) show that $L_\varepsilon \cong 0.93$ H. For a CBL topped by a finite inversion this value is little smaller and about 0.8 H (Schumann, 1991a). If the coherent motions are non-zero, the lengthscale is smaller because it measures the size of the turbulent parts only. Hunt et al. (1989) proposed to relate L_ε to the mean shear. In rough agreement with their proposal, we set

$$L_\varepsilon = 0.93 \left[H^{-1} + \sigma \frac{2}{w_*} \left\{ \left(\frac{u}{h}\right)^2 + \left(\frac{w}{b}\right)^2 \right\}^{1/2} \right]^{-1}. \qquad (51)$$

Here, 2u/h and 2w/b are the effective shear rates in the horizontal and vertical directions. The coefficient σ is to be adjusted empirically. Here we will present results for $\sigma = 1$. The results don't change significantly if we vary σ between 0.5 and 2. These approximations allow us to compute v′ from Eq. (49) for steady state, i.e. for de/dt = 0,

$$\frac{v'^3}{w_*^3} = (2/3)^{3/2} \frac{L_\varepsilon}{H} \left\{ \frac{1}{2} - \gamma \frac{u}{w_*} \frac{H}{w_*^2} \frac{du}{dt} (1 + 4H^2/\lambda^2) \right\}. \qquad (52)$$

From the solution v′, we can now determine the diffusivities as a function of the turbulence intensity, using Eq. (17). For u = 0, Eq. (52) predicts realistically a rms value $v' = [(2/3)^{3/2}\, 0.93/2]^{1/3}\, w_* \cong 0.633\, w_*$. The corresponding total energy is $E_{tot} = 0.6\, w_*^2$. In order to compare the results obtained in this section with those obtained in Section 4 for $\alpha = 0.05$, we use $\alpha = 0.05/0.633 = 0.079$. By this selection of α we obtain the same solutions for $u \to 0$. For increasing u, the turbulent part diminuishes because part of the heat flux is now carried by the coherent motion part. For larger values of u, v′ reaches a minimum and then increases because of increasing contributions by shear, both internally and by surface friction. This becomes more obvious if one inserts Eq. (36), which shows that for small u/w_*, the buoyancy part reduces about linearly with u, because part of the heat flux is transported by the coherent motion part. For larger velocity u, the shear part grows about quadratically with u. Hence, we expect that v′ decreases from $0.633\, w_*$ for $\lambda/H = 0$ down to a minimum value near λ_{max} and increases again for very large wavelengths. For $\delta = q = 0$, its value returns to that for zero wavelength, because, in such homogeneous cases, $u \to 0$ for $\lambda/H \to \infty$.

Iterative solutions of these equations require some underrelaxation which indicates that the steady state solution is prone to at least weak instabilities. Figure 5 shows the resultant turbulence intensities in terms of total kinetic energy and in terms of the individual components, for $\delta/H = 0.1$, $q = 0$. It should be noted that these results depend quite strongly on the model parameters, in particular on α and γ. Nevertheless, the numerical results are in agreement with the theoretical expectation. We see that v'^2, which approximates the total variance in the y direction, decreases with δ/H up to a broad minimum near δ/H of order five. The vertical velocity variance, computed as the sum of coherent and turbulent motions, shows a non-monotonic behaviour but decreases and reaches v'^2 for large wavelengths. Only the horizontal velocity variance shows a significant increase at $\lambda/H > 2$. However, this increase is not strong enough to prevent a slight reduction in total kinetic energy. The coherent motion amplitude stays finite for very large wavelengths because of the finite terrain undulation in this example. Therefore, for $\lambda/H \to \infty$, all energy components are smaller than for $\lambda = 0$.

Figures 6 and 7 show results for $\alpha = 0.079$ similar to those in Figures 3 and 4 for $\alpha = 0.05$, but now with variable turbulence intensity. Because of smaller v′ and, hence, reduced diffusivities, the peak amplitude of the coherent motions is larger than for fixed diffusivities. In comparison to the LES results, the curves do agree only slightly better. Hence, the model of Section 4 is about equally valid with respect to the mean coherent motions, but we cannot support the increase of the turbulence velocity scale as a function of friction velocity, see Eq. (19), which we adopted from Penc and Albrecht (1987). In contrary, our analysis suggests that the relevant turbulent scale decreases with increasing u_*/w_*, at least for small values of this ratio.

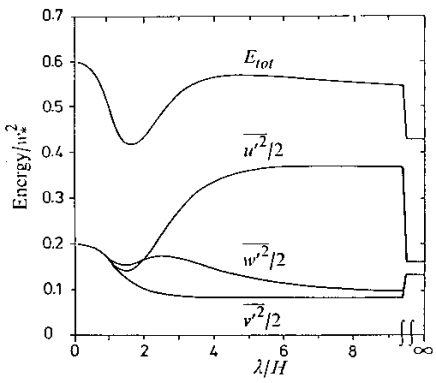

Figure 5 Total energy E_{tot}, and energies of the three velocity components. Lateral: $v'^2/2$, vertical: $v'^2/2 + \gamma w^2/2$, and horizontal: $v'^2/2 + \gamma u^2/2$, versus wavelength λ/H, for $q/Q = 0$, $\delta/H = 0.1$, $z_0/H = 10^{-4}$, $\alpha = 0.079$.

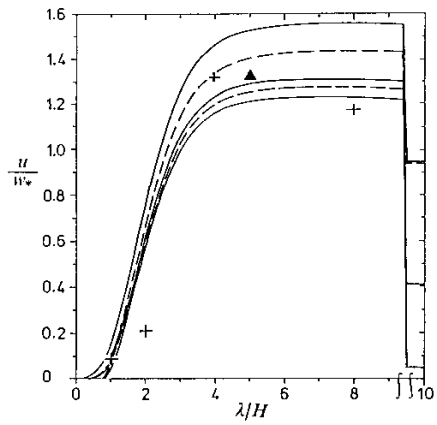

Figure 6 Same as Figure 3 but for variable turbulence fluctuations v′ and for $\alpha = 0.079$ (comparable to $\alpha = 0.05$ in Figure 3).

Finally, Figure 8 shows the motion amplitudes versus the inhomogeneity parameters for fixed wavelength and surface roughness values. The velocity u increases about linearly, compare Eq. (42). Again, we see that the undulated surface has stronger effects than an equivalent variation in the surface heating. The vertical velocity increases also but more slowly. The total kinetic energy stays close to constant but the turbulence velocity decreases slightly, as explained above. The friction velocity stays close to constant. The vertical velocity variance $v'^2 + \gamma w^2$ (not plotted) increases but slightly (by about 10 % in the parameter range of Figure 8).

If z_0/H is reduced by a factor of 100 (to 10^{-6}), then we obtain slightly (about 4 %) larger flow velocities and an about 30 % smaller friction velocity. An increase of z_0/H to 10^{-2} causes larger changes (20 % reduction in flow velocity and about 100 % increase in friction velocity). However, the qualitative trends remain unchanged.

6 Relationship between Heat Flux and Temperature Variations

The present theory applies for a given mean temperature flux Q with mean variations ± q/2. If these fluxes are unknown but if instead we know the mean temperature difference $\Theta = T(z_0) - (T_1 + T_2)/2$ between the surface temperature at roughness height (which still differs from the radiatively effective surface temperature, see Schumann, 1988) and the temperature within the lower mixed layer, and know the horizontal temperature variation, say its amplitude ϑ, at the surface, then we may estimate the convection from the present model if we know the dependence of the heat

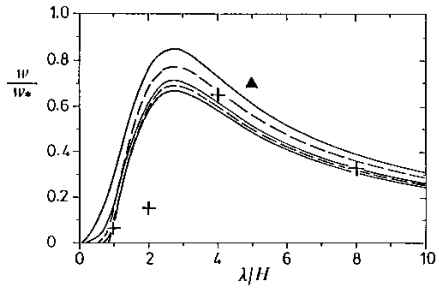

Figure 7 Same as Figure 4 but for variable turbulence fluctuations v′ and for $\alpha = 0.079$ (comparable to $\alpha = 0.05$ in Figure 4).

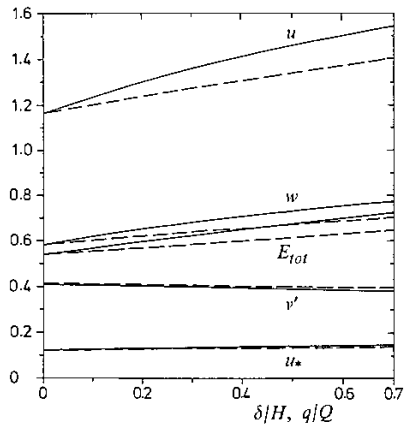

Figure 8 Circulation parameters versus inhomogeneity parameters δ/H (full curves) and q/Q (dashed curves) for $\lambda/H = 4$, $z_0/H = 10^{-4}$, $\alpha = 0.079$. The curves indicate the velocities of the coherent motions in horizontal direction (u/w_*), and in vertical direction (w/w_*), the total kinetic energy E_{tot}/w_*^2, turbulence velocity v'/w_*, and surface friction velocity u_*/w_*.

fluxes on the surface temperatures. It appears reasonable to assume that $\vartheta/\Theta = q/Q$, because the heat transfer, for the same flow field, is linear in the temperature differences. For zero mean wind and a coherent circulation over homogeneous surfaces, the mean heat flux is approximately related, according to Schumann (1988), by

$$Q = \Theta w_* [z_0/(10\,H)]^{1/3}, \tag{53}$$

or inversely,

$$w_* = (\beta g \Theta)^{1/2} H^{1/3} (z_0/10)^{1/6}. \tag{54}$$

This result allows one to evaluate u as a function of the external parameters from the present model for given surface temperature differences. It is an approximative result because the relationships used do not account for changes in the heat flux from variations in the coherent circulation.

Alternatively, we may evaluate the heat transfer as a function of the effective velocity at the surface and the local temperature differences using the local Monin-Obukhov functions as in Schumann (1988). The effective velocity is estimated as $u + 0.7\,v'$. This accounts for the fact that even for zero coherent motions the surface experiences fluctuating turbulent motions of amplitude $0.7\,v'$. The factor 0.7 has been justified empirically in Schumann (1988). Consequently, the following relationships are used to determine an effective friction velocity $\tilde{u}_*$, the related values of the temperature difference Θ, and the effective Obukhov lengthscale $\tilde{L}$:

$$\frac{\Theta \pm \vartheta/2}{\theta_*} = \frac{1}{\kappa}\left[\ln (z/z_0) - \psi_h (z/\tilde{L}) + \psi_h (z_0/\tilde{L})\right], \tag{55}$$

$$u + 0.7\,v' = \frac{\tilde{u}_*}{\kappa}\left[\ln (z/z_0) - \psi_m (z/\tilde{L}) + \psi_m (z_0/\tilde{L})\right], \tag{56}$$

$$\theta_* = \frac{Q \pm q/2}{\tilde{u}_*}, \quad \tilde{L} = -\frac{\tilde{u}_*^3}{\kappa \beta g (Q \pm q/2)}. \tag{57}$$

Here ψ_m was specified in Eq. (15) and

$$\psi_h(\zeta) = 2 \ln [(1 + \varphi_h^{-1})/2], \; \varphi_h(\zeta) = (1 - 16\zeta)^{-1/2}, \tag{58}$$

see Paulson (1970) and Dyer (1974).

Numerical evaluations of these equations have shown that the equivalence $\vartheta/\Theta = q/Q$ is valid indeed. Moreover, it has been found that the ratio of $\Theta(u)/\Theta(0)$ is close to unity for all values of the flow velocity u shown in Figure 6. Moreover, Θ is closely approximated by Eq. (53). We found that the mean temperature difference changes only very little with the wavelength. The maximum variation is 10 %. (We found a slight increase of Θ with increasing u which is a disturbing fact; it reflects limitations in the validity of the Monin-Obukhov relationships for $u < w_*$.) The weak variation of Θ is consistent with the LES results; Krettenauer and Schumann (1991) found an even smaller variation of 3 %. Hence, in the present case with zero mean wind, the heat flux is mainly controlled by the turbulent motions at the surface. The coherent motion part is less important.

7 Effective Diffusivities

In this section, first we estimate the effective vertical diffusivity K_V for heat transfer between the two lower and the two upper subdomains (not to be confound with K_v). The result will be compared to the effective diffusivity for turbulent fluxes through the bottom surface into the two lower subdomains, K_S. Secondly, the effective horizontal diffusivity K_H is discussed. Finally, we will deduce the vertical diffusivities, K_{up} and K_{down}, for bottom-up and top-down diffusion for a species emitted with a mean flux C and horizontal variation c either upwards at the bottom surface or downwards at the top boundary.

The mean vertical heat flux through the interface between the lower and upper subdomains equals Q/2. This flux is related to K_V by

$$\frac{Q}{2} = -K_V \frac{T_3 + T_4 - T_1 - T_2}{2h}. \tag{59}$$

The temperature difference is given by Eq. (34). Hence, we can evaluate K_V. The result is

$$K_V = \frac{H\,[w\,(u + u') + w'\,(u + 2u')]}{4u' + u\,(2 - \delta/H - q/Q)}. \tag{60}$$

For $\lambda/H \to 0$, or more generally for $u \to 0$, $w \to 0$, we have

$$K_V = K_v = w'\,H/2. \tag{61}$$

On the other hand, for $u' \ll u$,

$$K_V = \frac{(w + w')\,H}{2 - \delta/H - q/Q}. \tag{62}$$

Hence, K_V increases strongly with increasing amplitude of the coherent motions. We expect a maximum for $\lambda/H \cong 3$, where the vertical velocity achieves its maximum. For larger wavelengths, the diffusivity decreases. This is reasonable because any heat added to the lower subdomain is first transported with the mean circulation horizontally before it eventually is carried upwards. The larger the horizontal circulation wavelength, the slower will be the vertical mixing. We further observe an increase of vertical diffusivity with increasing inhomogeneity. This comes from increase in vertical velocity which enters the above expression explicitly and also by reducing the vertical temperature differences; the

latter causes the factor in the denominator. For $\lambda/H = 4$, we may apply Eq. (42) to estimate $w = uh/b$ so that

$$K_V \cong w_* H \frac{A}{4}\left(1 + \frac{\delta}{H} + \frac{3}{4}\frac{q}{Q}\right). \tag{63}$$

Figure 9 depicts the dependence of K_V, Eq. (60), on λ/H and on the inhomogeneity parameters. As to be expected from the above analysis, the diffusivity is small for $\lambda/H = 0$, and maximum near $\lambda/H \cong 3$. For very large wavelengths, it returns to the value for $\lambda/H = 0$ because of vanishing vertical mean velocity.

This result suggests a strong impact of inhomogeneities on vertical mixing. This is true with respect to internal mixing. However, the mixing from the surface into the CBL is controlled by small-scale turbulence which is much less affected by the coherent motions. From Eq. (53) we find the effective diffusivity at the surface

$$K_S = \frac{Q}{\Theta/h} = \frac{1}{2} w_* H \left(\frac{z_0}{10H}\right)^{1/3}. \tag{64}$$

As is the case for the friction velocity and for the surface temperature difference, this diffusivity is approximately independent of the coherent motion. For $z_0/H = 10^{-4}$, its value is $K_S/(w_* H) = 0.01$, whereas the internal mixing diffusivity K_V is much larger. Hence, the variation of diffusivity within the mixed layer is rather unimportant for vertical transports from the surface through the CBL.

Next, we determine the effective horizontal diffusivity which controls the heat flux, induced by the differential heating q, between the left subdomains (1 and 4) and the right ones (2 and 3). Here the mean horizontal flux is $-q\lambda/(8H)$. This flux grows infinitely with λ/H. The mean temperature gradient $(T_2 + T_3 - T_1 - T_4)/(2b)$ is given by Eq. (35). It is applied for $Q = 0$, because the flux is driven by that temperature gradient which is induced by q only. The result is

$$K_H = \frac{\lambda}{4}\frac{w(u+u') + w'(u+2u')}{w+2w'}. \tag{65}$$

Note that this diffusivity depends on the inhomogeneity parameters only indirectly by virtue of u and w. For very small wavelength or vanishing coherent motions, it equals $K_H = K_h = bu' = 3\alpha v' H/2$. For larger wavelength, however, its value increases up to infinity as $K_H \to \lambda u/8$. Such a large diffusivity is required to give finite temperature gradients for the growing lateral heat flux. For $u' \ll u$, $w' \ll w$, $K_H = \lambda u/4$. The ratio of horizontal to vertical diffusivities is $K_H/K_V \cong \lambda^2/(4H^2)$ for such conditions and small inhomogeneity. For $\lambda = 4H$ we obtain $K_H \cong 4K_V$ and

$$K_H \cong w_* H A\,[1 + \delta/(2H) + q/(4Q)]. \tag{66}$$

It is reasonable to expect that K_H/K_V is larger than $K_h/K_v \cong 3$, because the small-scale turbulence is more isotropic than the large-scale coherent motion. Note that the same model implies $K_H = K_h$ at the lateral sides of the domain sketched in Figure 2. Therefore, a species which is diffused laterally over several convection cells will experience a considerably smaller horizontal diffusivity. The present model would give $2(K_h^{-1} + K_H^{-1})^{-1}$ for this parameter, but this does not account for three-dimensional flow between various convection cells.

Finally, we compute the diffusivities for vertical transport of a scalar which is emitted with mean flux C and horizontal variability c, as corresponding to Q and q. For bottom-up diffusion, i.e. for given surface fluxes and zero fluxes at the top of the boundary layer, the budget equations for the species concentrations c_i in the four domains are formally the same as those for the temperatures T_i. Hence, the resultant concentrations can be read from Eqs. (29) to (32) with T_i, Q, q replaced by c_i, C, c, respectively. We obtain

$$K_{up} = \frac{H[w(u+u') + w'(u+2u')]}{4u' + u(2 - \delta/H - c/C)}. \tag{67}$$

Note the formal similarity to K_v, Eq. (60), as expected. However, we now see more clearly that the inhomogeneity q/Q affects the diffusivity only by means of the velocities u and w. For $u' \ll u$, $w' \ll w$, we have

$$K_{up} = \frac{Hw}{2 - \delta/H - c/C}. \tag{68}$$

For $\lambda/H = 4$, using Eq. (42), this gives

$$K_{up} \cong w_* H \frac{A}{4}\left(1 + \frac{\delta}{H} + \frac{q}{4Q} + \frac{c}{2C}\right). \tag{69}$$

For the top-down diffusion case, we assume that the fluxes are imposed at the top boundary, simulating

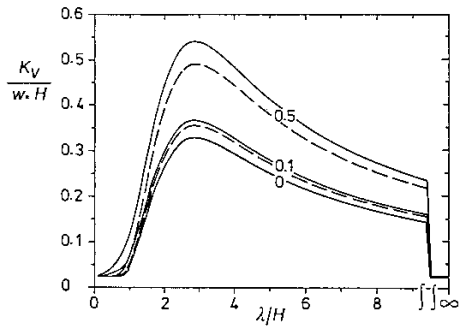

Figure 9 Vertical effective diffusivity $K_v/(w_* H)$ versus wavelength λ/H for various values of terrain amplitude $\delta/H = 0, 0.1$, and 0.5, with $q/Q = 0$ (full curves), and for various values of surface heating $q/Q = 0$, 0.1, and 0.5, with $\delta/H = 0$ (dashed curves). Asymptotic solutions for $\lambda/H = 1000 \cong \infty$ are indicated at the right vertical axis; $z_0/H = 10^{-4}$, $\alpha = 0.079$.

entrainment flux from above the inversion. The flux C is taken positively downwards; the variation c is positive if the flux into subdomain 3 is larger than into subdomain 4, depicted in Figure 2. In this case, we have to start from slightly changed budget equations, similar to those in Eqs. (4) to (7). One quickly notes that the changes affect the source terms only. Therefore, the solutions are formally the same as given by Eqs. (29) to (32), with T_i replaced by c_i, and changed definitions of the W_i:

$$W_1 = -\frac{\{1 + \delta/(2H)\}\, C}{2\,(w + w')}, \tag{70}$$

$$W_2 = -\frac{b\,\{1 - \delta/(2H)\}\, C}{2h\,(u + u')}, \tag{71}$$

$$W_3 = -\frac{\{1 + \delta/(2H) + c/C\}\, C}{2\,(w + w')}, \tag{72}$$

$$W_4 = -\frac{b\,\{1 - \delta/(2H) - c/C\}\, C}{2h\,(u + u')}. \tag{73}$$

From these solutions we evaluate $K_{down} = Ch/(c_3 + c_4 - c_1 - c_2)$, which results in

$$K_{down} = H\,\frac{w\,(u + u') + w'\,(u + 2u')}{4u' + u\,(2 + \delta/H + c/C)}. \tag{74}$$

For $u' \ll u$, $w' \ll w$, and $\lambda = 4\,H$, one obtains

$$K_{down} \cong w_* H\,\frac{A}{4}\left(1 + \frac{q}{4Q} - \frac{c}{2C}\right). \tag{75}$$

We see that the bottom-up diffusivity is larger than the top-down diffusivity over undulated terrain. This is a consequence of the asymmetry of the flow structure. For bottom-up diffusion the species is transported first with the shorter updraft while for top-down diffusion the species is transported first with the longer downdraft. The bottom-up diffusivity is also larger than its top-down counterpart if $c > 0$. This is caused by the fact that the extra flux c is added into the upward branch of the circulation from below (subdomain 2) but into the horizontal branch from above (subdomain 3). This topological asymmetry drops if the sign of c is changed at one of the boundaries. For $\delta = c = 0$, i.e. for homogeneous surfaces, the present model gives equal values for both kinds of diffusion. This is, as we will discuss below, not realistic, but a consequence of the symmetric flow structure which is assumed in this model.

8 Conclusions

The simple model described in this paper gives quasi analytical solutions which approximately predict the amplitude of coherent convective circulations together with turbulent mixing over homogeneous and over inhomogeneous surfaces with variable surface heigth $\delta/H < 1$ and variable surface heat flux $q/Q < 1$ and (which has been shown to be equivalent) variable surface temperature. Under the condition of zero mean wind and for a CBL capped by a strong inversion, we have shown that the dominant scales of convection over homogeneous surfaces are of the order 2 to 4 H. At these wavelengths, inhomogeneities from variable surface heat flux and from surface undulation have about equivalent effects if $\delta/H = q/(2Q)$; for large wavelengths, the equivalence is given for $\delta/H = q/Q$. Surface inhomogeneities cause a weak increase in the mean circulation intensity, however, at the expense of smaller turbulent fluctuations.

Certainly, the model cannot provide more than order of magnitude estimates because of all its simplifications. Nevertheless, it is surprising to see how well such a model compares to the LES results and to findings from observations even in the quantitative sense. This reflects the fact that the structure of the CBL is controlled by the most energetic large-scale circulation which can be represented even in two dimensions and resolved with just four grid cells. Moreover, the motion amplitude adjusts such that it carries the right amount of heat from the surface into the fluid layer. This process is controlled by the heat input at the surface but otherwise only weakly dependend on small-scale turbulent mixing. For a given surface heat flux the details of the heat transfer process get unimportant for the internal dynamics. Instead, the motion amplitude depends only on the square root of the turbulent diffusivities whereas the onset of laminar convection, as given by the critical Rayleigh number (see the Appendix), for given heat flux, scales with the third power of the diffusivities. This explains why a very coarse resolution suffices. With respect to surface friction the sensitivity is even weaker because the surface friction velocity is much smaller than the convective velocity scale. However, surface roughness does control the surface temperature difference, which varies approximately with $(z_0/H)^{1/3}$.

The model shows that the coherent and the turbulent motions compete for the given buoyancy forcing. For increasing coherent motions, buoyant production rate of smaller scales gets reduced. The shear induced by the coherent motions does enhance small-scale turbulence but at the same time reduces the turbulent lengthscales and hence increases the dissipation rate of turbulent motions. For these reasons the turbulence intensity will most likely decrease over inhomogeneous terrain with more pronounced coherent motion parts. The contribution of coherent motion to the total vertical velocity variance is small at large wavelengths. This explains why Schmidt (1988) and Graf and Schumann (1991) found a slight decrease of vertical velocity fluctuations for variable surface heating. The results show that the convection responses to inhomogeneities most strongly near the internal scale of convection over homogeneous terrain. Hence the model also explains why Kret-

tenauer and Schumann (1991) found a "resonant" response to undulated terrain at wavelengths of the order 4 H. Moreover, the weak impact of surface undulations on the total kinetic energy is consistent with what their LES has given.

When the model is applied for laminar flow, see Appendix, it predicts a critical Rayleigh number of 384 instead of the exact value 720. This is not far off in view of the fact that the Rayleigh number depends on the fourth power of lengthscales. Moreover, we have estimated the value of the critical Reynolds number, which is about 50 and independent of the Prandtl number, by comparing laminar and turbulent solutions. Krettenauer and Schumann (1989b, 1991) found turbulent solutions from direct numerical simulations for Re = 100; they did not test at smaller Reynolds numbers. Hence, this estimate is again consistent with previous results. The strong difference between the critical wavelength for the onset of laminar convection and that of maximum nonlinear convective response, both in the laminar and turbulent model, is of theoretical interest (Fiedler, 1989). It explains the weak sensitivity of turbulent convection to the type of thermal boundary condition at the surface (Krettenauer and Schumann, 1989a).

Although the applicability of diffusion concepts is questionable for flows with strong coherent motion parts (Ebert et al., 1989), it is nevertheless interesting to estimate their magnitude and to analyse their dependence on the coherent motions. The model reveals the rather strong importance of surface inhomogeneities for vertical and horizontal mixing of species introduced into the interiour of the CBL. For a homogeneous surface, the effective vertical diffusivity is $K_V/(w_* H) \cong 0.3$ for mixing between the lower and upper part of the mixed layer over a homogeneous surface. Because of larger horizontal flow velocity and increasing mixing lengthscale, the ratio of horizontal to vertical diffusivities within a convection cell grows with the square of λ/H. However, it remains open how far this result applies to lateral exchange between various convection cells, which is poorly represented in the present two-dimensional model. On the other hand, the inhomogeneities have weak effect on mixing from the surface into the CBL.

As shown by Wyngaard and Weil (1991) and others, a species introduced through an area source at the layer top and having zero flux through the bottom (i.e., one undergoing "top-down" diffusion) has a well-behaved eddy diffusivity with maximum value of about 0.2 $w_* H$ (Schumann, 1989). But one introduced at the bottom, with zero flux at the top ("bottom-up" diffusion) has a much different diffusivity profile. It may show a singularity with very large or negative values but is otherwise of order 0.4 $w_* H$ (Schumann, 1989). This transport asymmetry is caused in the CBL by the skewed turbulence structure composed of strong updrafts which shrink in mean cross-section with altitude within the mixed layer, and are surrounded by weak and wide downdrafts. The present model gives about the correct magnitude of the diffusivity but, since this asymmetry is not included, it does not predict differences between bottom-up and top-down diffusion for homogeneous cases. Some further analysis (the details are omitted here for brevity, see Schumann 1991b) with a model that assumes different widths for the updraft and downdraft parts instead of b still does not explain this asymmetry, whereas a model which assumes a vertical variation in the width of the updraft and downdraft parts does. However, the present model predicts asymmetry between bottom-up and top-down diffusion for a passive species when the bottom surface is undulated. Hence, an asymmetry of geometrical nature has similar effects as an asymmetry of dynamical nature.

It should be noted that the large-scale coherent motions require long times to reach a steady circulation. The time scales of the present model can be read from Eqs. (4) to (7) and (23). The largest time scales are those to reach thermal equilibrium (of order $b/u' + h/w'$) whereas those for velocity are smaller in this model (of order $(2h)/(2u'h^3/b^3 + 4w' + C_d\, u_*)$) because of continuity and imposed symmetry. From LES we know that steady state is reached after a time of about 6 H/w_* for $\lambda/H \cong 4$, which amounts to more than one hour for typical scale values in the atmosphere. The time scale increases with λ/H. The mean circulation cannot fully develop if the flow passes over the surface wave within a time interval shorter than the time in which the circulation develops. Hence, the mean wind U must be small in comparison to w_* to establish strong circulations and to make the present theory applicable. Otherwise, the reactions to surface variations will be smaller than predicted by the present model. However, the effects of inhomogeneities should be notable at smaller spatial scales with shorter time scales (e.g. by triggering local thermals or bubbles), which are not resolved by the simple model. Such local motions have been observed by Reinhardt (1985). He reported about bursts at the edges of forest areas surrounded by cultured acres.

The present model shows that the structure of the CBL is mainly controlled by its mean depth and the mean surface heat flux. With the exception of internal mixing, variations in these parameters at scales smaller than the depth of the boundary layer are of small importance with respect to the motions in the CBL. The surface roughness has little dynamical effect on the structure of the CBL but strongly influences the relation between heat flux and temperature at the surface. Perhaps, future studies provide similarly simple models for cases

with strong mean wind, including the effects of nonzero momentum and heat exchange at the top of the boundary layer.

Appendix
Laminar Solutions and Critical Rayleigh and Reynolds Number

The model given in Section 2 applies to laminar flow with viscosity ν and conductivity γ if we set $u' = \nu/b$, $w' = \nu/h$, and $u_*^2 = 2\nu u/h$ in the momentum balances, Eqs. (9) to (13), and set $u' = \gamma/b$, $w' = \gamma/h$ in the heat balances, Eqs. (4) to (7). The resultant equations have solutions similar to those given in Sections 3 and 4, in particular

$$(4h^4/b^4 + 6)\,\nu u/h = \frac{w_*^3\,[2w + (w + 2\gamma/h)\,(\delta/H + q/Q)]}{8\,[w\,(u + \gamma/b) + (u + 2\gamma/b)\,\gamma/h]} + \frac{w_*^3\,[4\gamma/b + u\,(2 - \delta/H - q/Q)]\,\delta/\lambda}{8\,[w\,(u + \gamma/b) + (u + 2\gamma/b)\,\gamma/h]}. \quad (76)$$

If one evaluates this equation for small convective velocities, i.e. for $u \ll \nu/h$ and $w \ll \nu/b$, for homogeneous surfaces, one finds that positive velocities develop only if the Rayleigh number Ra exceeds a critical value which depends on the wavelength,

$$\mathrm{Ra} \equiv \frac{\beta g Q H^4}{\nu \gamma^2} > 64\,(6 + 64\,H^4/\lambda^4)\,. \quad (77)$$

Hence, laminar convection sets in first at infinite wavelength λ at a critical Rayleigh number

$$\mathrm{Ra}_{\mathrm{crit}} = 384\,. \quad (78)$$

Krettenauer (1991) deduced the critical conditions from solving the exact laminar equations. He found also that convection starts first at infinite wavelength and computed $\mathrm{Ra}_{\mathrm{crit}} = 720$.

Limiting solutions over inhomogeneous terrain for laminar flow are

$$\frac{u}{w_*} = \sqrt{\frac{1}{48}\frac{w_* H}{\nu}\left(\frac{\delta}{H} + \frac{q}{Q}\right)}\,, \quad \text{for } \frac{\lambda}{H} \to \infty\,, \quad (79)$$

$$\frac{w}{w_*} = \frac{w_*^2 H\lambda}{32\nu\gamma}\frac{H^3}{\lambda^3}\left\{\frac{\delta}{H} + \frac{q}{Q} + 4\frac{\delta H}{\lambda^2}\right\}, \quad \text{for } \frac{\lambda}{H} \to 0\,. \quad (80)$$

In the latter result, the terms including δ must go to zero for $\lambda \to 0$, which is the case for a sufficiently smooth terrain. The limiting results in Eqs. (78) to (80) remain unchanged if diffusion along the flow direction is included in the model.

For laminar flow, evaluations of the equations show that w achieves its maximum at about $h = b$ ($\lambda = 2H$), with $u' \ll u$ and $w' \ll w$. For this case, one obtains

$$\frac{u}{w_*} = \frac{w}{w_*} = \frac{w_* H}{80\nu}\sqrt{1 + \frac{\delta}{H} + \frac{q}{2Q} - \frac{\delta}{4H}\left(\frac{\delta}{H} + \frac{q}{Q}\right)}\,. \quad (81)$$

It is interesting to note that this solution is independent of the Prandtl number ν/γ. The amplitude of the laminar solution exceeds that of the turbulent case, see Eq. (42), if

$$\mathrm{Re} = \frac{w_* H}{\nu} > 80\,A > 56\,. \quad (82)$$

Hence, it appears reasonable to expect that the convection becomes turbulent if the Reynolds number Re exceeds a critical value of order 50.

The analysis shows that the critical wavelength for the onset of laminar convection (which is infinite and controlled by molecular diffusivity) is much different from the wavelength where the largest amplitude of motions occur at supercritical Rayleigh numbers. The latter is of order H and only weakly dependent on the diffusivities. A similar conclusion has been obtained, from a continuum analysis, by Fiedler (1989). It is well known that the critical wavelength for the onset of laminar convection is finite and of order H if the bottom boundary condition prescribes constant temperature instead of constant heat flux. In this case, turbulent convection shows maximum intensity also at about the same wavelength. These findings explain why the scales of turbulent motions for convection are about the same over surfaces with prescribed heat flux and surfaces with prescribed temperature, as has been shown by LES of such cases in Krettenauer and Schumann (1989a).

References

Becker, F., H.-J. Bolle and *P. R. Rowntree*, 1988: The International Satellite Land-Surface Climatology Project. ISLSCP-Report No. 10. ISLSCP-Secretariat, FU Berlin, Inst. f. Meteorologie, Berlin 41.

Caughey, S. J. and *S. G. Palmer*, 1979: Some aspects of the turbulent structure through the depth of the convective boundary layer. Q. J. R. Met. Soc., **105**, 811–827.

Druilhet, A., J. Noilhan, B. Benech, G. Dubosclard, D. Guedalia and *J. Frangi*, 1983: Étude expérimentale de la couche limite au-dessus d'un relief modéré proche d'une chaîne de montagne. Boundary-Layer Met., **25**, 3–16.

Dyer, A. J., 1974: A review of flux-profile relationships. Boundary-Layer Met., **7**, 363–372.

Ebert, E. E., U. Schumann and *R. B. Stull*, 1989: Nonlocal turbulent mixing in the convective boundary layer evaluated from large-eddy simulation. J. Atmos. Sci., **46**, 2178–2207.

Egger, J., 1987: Simple models of the valley-plain circulation. Part I: Minimum resolution model. Meteor. Atm. Phys., **36**, 231–242.

Fiedler, B. H., 1989: Scale selection in nonlinear thermal convection between poorly conducting boundaries. Geophys. Astrophys. Fluid Dyn., **46**, 191–201.

Garrat, J. R., R. A. Pielke, W. F. Miller and *T. J. Lee*, 1990: Mesoscale model response to random, surface based perturbations – a sea-breeze experiment. Boundary-Layer Met., **52**, 313–334.

Graf, J. and *U. Schumann*, 1991: Simulation der konvektiven Grenzschicht im Vergleich mit Flugzeugmessungen beim LOTREX-Experiment. Meteorol. Rdsch., **43**, 140–148.

Hadfield, M. G., 1988: The response of the atmospheric convective boundary layer to surface inhomogeneities. Colorado State University, Atmospheric Science Paper No. 433.

Hechtel, L. M., C.-H. Moeng and *R. B. Stull*, 1990: The effects of nonhomogeneous surface fluxes on the convective boundary layer: A case study using large-eddy simulation. J. Atmos. Sci., **47**, 1721–1741.

Hunt, J. C. R., P. Moin, R. D. Moser, P. Spalart, M. N. Mansour, J. C. Kaimal and *E. Gaynor*, 1989: Cross correlation and length scales in turbulent flows near surface. In H.-H. Fernholz and H. E. Fiedler (Ed.): Advances in Turbulence 2, p. 128–134, Springer, Berlin.

Huynh, B. P., C. E. Coulman and *T. R. Turner*, 1990: Some turbulence characteristics of convectively mixed layers over rugged and homogeneous terrain. Boundary-Layer Met., **51**, 229–254.

Jochum, A., 1988: Turbulent transport in the convective boundary layer over complex terrain. Proc. Eighth Symposium on Turbulence and Diffusion, San Diego, Americ. Meteorol. Soc., Boston, Mass., p. 417–420.

Kaimal, J. C., R. A. Eversole, D. H. Lenschow, B. B. Stankow, P. H. Kahn and *J. A. Businger*, 1982: Spectral characteristics of the convective boundary layer over uneven terrain. J. Atmos. Sci., **39**, 1098–1114.

Kelly, R. E. and *D. Pal*, 1978: Thermal convection with spatially periodic boundary conditions: resonant wavelength excitation. J. Fluid Mech., **86**, 433–456.

Krettenauer, K., 1991: Numerische Simulation turbulenter Konvektion über gewellten Flächen. Diss. Techn. Univ. Munich, report DLR-FB 91-12 (DLR Oberpfaffenhofen), 162 pp.

Krettenauer, K. and *U. Schumann*, 1989a: Struktur der konvektiven Grenzschicht bei verschiedenen thermischen Randbedingungen. Deutsche Meteorologen-Tagung, Deutscher Wetterdienst, Offenbach: Ann. Meteor., **26**, 278–279.

Krettenauer, K. and *U. Schumann*, 1989b: Direct numerical simulation of thermal convection over a wavy surface. Meteorol. Atmos. Phys., **41**, 165–179.

Krettenauer, K. and *U. Schumann*, 1991: Numerical simulation of thermal convection over a wavy surface. J. Fluid Mech., in print.

Moeng, C.-H. and *U. Schumann*, 1991: Composite structure of plumes in stratus-topped boundary layers. J. Atmos. Sci., **48**, 2280–2291.

Paulson, C. A., 1970: The mathematical representation of wind speed and temperature profiles in the unstable atmospheric surface layer. J. Appl. Meteorol., **9**, 857–861.

Penc, R. S. and *B. A. Albrecht*, 1987: Parametric representation of heat and moisture fluxes in cloud-topped mixed layers. Boundary-Layer Met., **38**, 225–248.

Priestley, C. H. B., 1962: The width-height ratio of large convective cells. Tellus, **14**, 123–124.

Ray, D., 1965: Cellular convection with nonisotropic eddys. Tellus, **17**. 434–439.

Reinhardt, M. E., 1985: Fallstudien zu Flugzeugmessungen entlang einer Tiefflugstrecke südlich von München. In J. M. Hacker and A. M. Jochum (Ed.): Workshop MEMO'84, DFVLR-Mitt. 85-04 (DLR Oberpfaffenhofen), p. 69–79.

Schädler, G., 1990: Triggering of atmospheric circulations by moisture inhomogeneities of the earth's surface. Boundary-Layer Met., **51**, 1–29.

Schmidt, H., 1988: Grobstruktur-Simulation konvektiver Grenzschichten. Diss. Univ. Munich, report DFVLR-FB 88-30 (DLR Oberpfaffenhofen), 143 pp.

Schmidt, H. and *U. Schumann*, 1989: Coherent structure of the convective boundary layer as derived from large-eddy simulations. J. Fluid Mech., **200**, 511–562.

Schumann, U., 1988: Minimum friction velocity and heat transfer in the rough surface layer of a convective boundary layer. Boundary-Layer Met., **44**, 311–326.

Schumann, U., 1989: Large-eddy simulation of turbulent diffusion with chemical reactions in the convective boundary layer. Atmos. Environm., **23**, 1713–1727.

Schumann, U., 1991a: Subgrid length-scales for large-eddy simulation of stratified turbulence. Theor. Comput. Fluid Dyn. (1991), **2**, 279–290.

Schumann, U., 1991b: Simulations and parametrizations of large eddies in convective atmospheric boundary layers. Proc. ECMWF Workshop on Fine-scale Modelling and the Development of Parametrization Schemes, Reading, in press.

Schumann, U. and *C.-H. Moeng*, 1991a: Plume fluxes in clear and cloudy convective boundary layers. J. Atmos. Sci., **48**, 1746–1757.

Schumann, U. and *C.-H. Moeng*, 1991b: Plume budgets in clear and cloudy convective boundary layers. J. Atmos. Sci., **48**, 1758–1770.

Spalding, D. B., 1972: A novel finite difference formulation for differential expressions involving both first and second derivatives. Int. J. Num. Meth. Engrg., **4**, 551–559.

Stull, R. B., 1988: An Introduction to Boundary Layer Meteorology. Kluwer, Dordrecht, 664 pp.

Tsvang, L. R., M. M. Fedorov, B. A. Kader, S. L. Zubkovskii, T. Foken, S. H. Richter and *Ya. Zeleny*, 1991: Turbulent exchange over a surface with chessboard-type inhomogeneities. Boundary-Layer Met., **55**, 141–160.

Walko, R. L., W. R. Cotton and *R. A. Pielke*, 1990: Large eddy simulation of the CBL over hilly terrain. Proc. 9th Symposium on turbulence and diffusion. Roskilde, Denmark, American Meteorol. Soc., Boston, Mass., p. 409–412.

Wilczak, J. M. and *M. S. Phillips*, 1986: An indirect estimation of convective boundary layer structure for use in pollution dispersion models. J. Clim. Appl. Met., **25**, 1609–1624.

Wyngaard, J. C. and *J. C. Weil*, 1991: Transport asymmetry in skewed turbulence. Phys. Fluids, **A 3**, 155–162.